ОБЪЕДИНЕННЫЙ
ИНСТИТУТ
ЯДЕРНЫХ
ИССЛЕДОВАНИЙ
ДУБНА

E17 - 9518

A.Holas

NUMERICAL INTEGRATION OVER THE SOLID ANGLE AND VOLUME OF THE BRILLOUIN ZONE

1976

E17 - 9518

A.Holas*

NUMERICAL INTEGRATION OVER THE SOLID ANGLE AND VOLUME OF THE BRILLOUIN ZONE

Submitted to "Journal of Computational Physics"

* Permanent address: Institute of Nuclear Research, Swierk, 05-400 Otwock, Poland.

1. *INTRODUCTION*

The essential step in many solid state physics calculations is the evaluation of integrals over solid angle or over volume in the appropriate regions defined by the symmetry of a crystal. (Brillouin Zones - BZ). The papers[1] and[2] give some examples of such problems in connection with thermodynamic properties of crystals, while papers[3] and[4] - in connection with electronic properties. All the methods of numerical integration developed and used in the mentioned papers exhibit some disadvantages. First of all, each of them is confined to that asymmetry of the crystal, to which it was designated and their extension to other symmetries is very difficult or impossible. They need elaborate programming, since their algorithms involve a great number of special cases connected with subzones and symmetrical positions of some points (e.g., ref. [2]). Almost all of those methods are slowly convergent, because a widely used uniform distribution of sampling points assures that only the first-degree polynomials are integrated exactly.

As it will be shown below, the methods proposed by us are free of those disadvantages.

2. *INTEGRATION OVER THE SOLID ANGLE*

2.1. *General Formula*

We are concerned here with the evaluation of the direction average

$$\langle f \rangle = \frac{1}{4\pi} \int_{4\pi} d^2\Omega \cdot f(\hat{\vec{r}}) \qquad (1)$$

of the function f depending on direction cosines

$$\hat{\vec{r}} = (\hat{x}, \hat{y}, \hat{z}) = \vec{r}/|\vec{r}| . \qquad (2)$$

If the function f possesses the crystal symmetry, then instead of the integration over the full 4π-steradian angle (1), it is enough to integrate f over the symmetry-irreducible solid angle Ω_{ir}, so

$$\langle f \rangle = \frac{1}{\Omega_{ir}} \int_{\Omega_{ir}} d^2\Omega \cdot f(\hat{\vec{r}}). \qquad (3)$$

Typical symmetry-irreducible angle is a trihedral solid angle, which may be characterized by the three vectors $\vec{Q}_1$, $\vec{Q}_2$, $\vec{Q}_3$ along its edges OA', OB', OC' (see *Fig. 1*). In the examples given below we shall define the vectors $\vec{Q}_i$ for some commonly used high symmetry crystals (for lower symmetries the irreducible angle may not be a trihedral one, but it can always be represented by the sum of few trihedral angles).

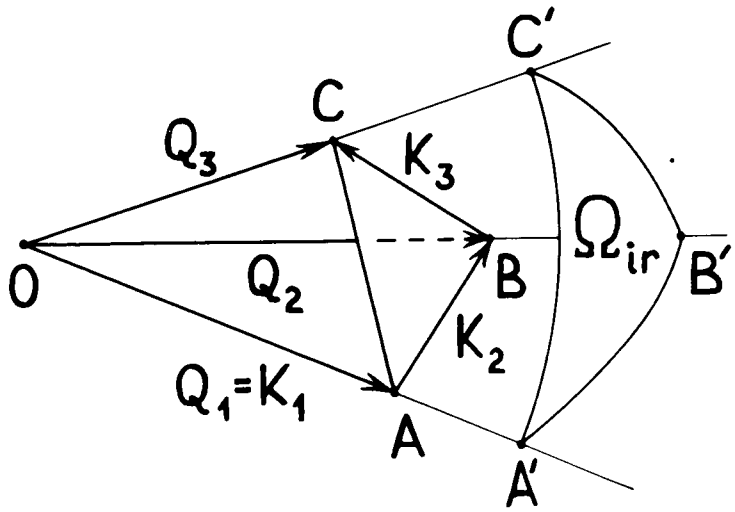

Fig. 1. A typical trihedral solid angle and an elementary tetrahedron of BZ.

According to the definition the element of the solid angle $d^2\Omega$ may be expressed by means of the element of the surface d^2S_n laying at the distance $|\vec{r}|$ and normal to $\vec{r}$:

$$d^2\Omega = d^2S_n/\vec{r}^{\,2}. \qquad (4)$$

Using the element $d^2\vec{S}$ of the surface other than normal, one should project it on the direction of the radius $\vec{r}$:

$$d^2\Omega = \left|\frac{d^2\vec{S}}{r^2} \cdot \frac{\vec{r}}{r}\right| . \qquad (5)$$

So by (5) the problem of solid angle integration is transformed to the surface integration.

In order to apply this transformation to the integral (3) we intersect the angle Ω_{ir} by the plane ABC (see *Fig. 1*) going through the ends of the vectors $\vec{Q}_1$, $\vec{Q}_2$, $\vec{Q}_3$. If we define vectors $\vec{K}_i$ as:

$$\vec{K}_1 = \vec{Q}_1, \quad \vec{K}_2 = \vec{Q}_2 - \vec{Q}_1, \quad \vec{K}_3 = \vec{Q}_3 - \vec{Q}_2 \qquad (6)$$

then any point of the surface ABC may be expressed in terms of them (see *Fig. 1*):

$$\vec{r} = \vec{K}_1 + \eta\vec{K}_2 + \zeta\vec{K}_3 \qquad (7)$$

and surface element, also

$$d^2\vec{S} = (\vec{K}_2 \times \vec{K}_3)d\eta\, d\zeta . \qquad (8)$$

In this way (3) may be rewritten as

$$\langle f \rangle = \frac{1}{\Omega_{ir}} \int_0^1 d\eta \int_0^{\eta} d\zeta\, w(\eta, \zeta)\, f(\hat{\vec{r}}(\eta, \zeta)), \qquad (9)$$

where the weighting function w according to (5), (8) and (7) equals

$$w(\eta, \xi) = |\vec{K}_1 \cdot (\vec{K}_2 \times \vec{K}_3)| / r^3. \qquad (10)$$

So we reduced the problem of the integration over the irreducible solid angle to the integration over the triangle with vertices (0,0), (0,1) and (1,1) in the space of variables (η, ξ). The variable transformation (7) and weighting function (10) are very easy to program and practically no time consuming because they involve only one square-root routine besides the elementary arithmetic operations.

As regards the integration over the triangle, there exist numerical methods which allow one to do it with high efficiency. In all the examples given in our paper we use integration formulae given by Hammer et al. (ref. /5/, pages 135, 136) which hold exactly for polynomials of at most degree N_{deg} (given there for $N_{deg} = 1,2,3$ and 5), and represent the integral as the sum of weighted integrands, over a set of N_p points ($N_p = 1,3,4$ and 7, respectively) affine-symmetrically distributed over the triangle:

$$\int_\Delta d\eta\, d\zeta\, \phi(\eta, \zeta) = \sum_{i=1}^{N_p} v_i\, \phi(\eta_i, \zeta_i). \qquad (11)$$

If higher accuracy is necessary, we decompose the triangle into $(N_{div})^2$ equal subtriangles and apply Hammer's formula to each subtriangle separately.

The above-demonstrated method of reducing the solid angle integral (3) to the two-dimensional integral over the triangle (9), though it is very simple, is not the only one, and, perhaps, not the best one. In principle, it is possible that another transformation would give smoother weighting function and therefore would be convergent more rapidly. General investigation of this question is rather difficult, therefore we confine ourselves to the derivation of another transformation based on spherical coordinates. Unfortunately, this approach is not so general as the previous one, and the derivation must be done separately for each symmetry considered, though in similar ways.

2.2. *Application to Some Structures. Spherical Coordinate Approach.*

2.2.1. Cubic Crystals

The symmetry-irreducible angle equals

$$\Omega_{ir} = 4\pi/48 \qquad (12)$$

and may be characterized by vectors:

$$\vec{Q}_1 = (1, 0; 0),\ \vec{Q}_2 = (1, 1, 0)/2^{1/2},\ \vec{Q}_3 = (1, 1, 1)/3^{1/2} \qquad (13)$$

in accordance with the usual definition of symmetry axes.

Passing to the second method of integration, we introduce the spherical coordinates:

$$\hat{x} = \sin\theta \cdot \cos\phi,\ \hat{y} = \sin\theta \cdot \sin\phi,\ \hat{z} = \cos\theta \qquad (14)$$

in terms of which (3) may be rewritten as

$$\langle f \rangle = \frac{1}{\Omega_{ir}} \int_0^{\pi/4} d\phi \int_{\theta_0(\phi)}^{\pi/2} d\theta \cdot \sin\theta \cdot f(\hat{\vec{r}}), \qquad (15)$$

where integration limit $\theta_0(\phi)$ is defined by the condition $\hat{y} = \hat{z}$, i.e.,

$$t_0(\phi) = \cos(\theta_0(\phi)) = \sin\phi/(1 + \sin^2\phi)^{1/2}. \qquad (16)$$

By transformation

$$t = \cos\theta \qquad (17)$$

eq. (15) receives the form of the integral over the triangle with one side being curvolinear:

$$\langle f \rangle = \frac{1}{\Omega_{ir}} \int_0^{\pi/4} d\phi \int_0^{t_0(\phi)} dt\, f(\hat{\vec{r}}). \qquad (18)$$

Further variable transformation from (ϕ, t) to (η, ζ):

$$\eta = 2^{1/2}\sin\phi,$$
$$\zeta = t\cdot\dot{\eta}(\phi)/t_0(\phi) \qquad (19)$$

changes (17) to integral over the usual triangle, i.e., to (9) exactly, with weighting function

$$w(\eta,\zeta) = (4-\eta^4)^{-1/2}. \qquad (20)$$

Transformation reciprocal to (19) and (17):

$$\sin\phi = \eta/2^{1/2},$$
$$\cos\theta = \zeta/(2+\eta^2)^{1/2} \qquad (21)$$

allows one to express $\hat{\vec{r}}$ (14) as a function of (η,ζ).

2.2.2. Tetragonal Crystals

The symmetry irreducible angle equals

$$\Omega_{ir} = 4\pi/16. \qquad (22)$$

and is characterized by vectors

$$\vec{Q}_1 = (1,0,0),\ \vec{Q}_2 = (1,1,0)/2^{1/2},\ \vec{Q}_3 = (0,0,1) \qquad (23)$$

if z axis is taken as the 4-fold one.

As in the cubic case, we derive here the formula (9) also using the spherical transformation. Introducing the spherical coordinates it will be convenient now to choose y -axis as the polar axis:

$$\hat{z} = \sin\theta\cdot\cos\phi,\ \hat{x} = \sin\theta\cdot\sin\phi,\ \hat{y} = \cos\theta. \qquad (24)$$

By applying the transformation (24) and (17), eq. (3) becomes:

$$\langle f\rangle = \frac{1}{\Omega_{ir}}\int_0^{\pi/2} d\phi \int_0^{t_0(\phi)} dt\, f(\hat{\vec{r}}), \qquad (25)$$

where $t_0(\phi)$ is defined by the condition $\vec{x}=\vec{y}$, which leads to the same relation as previously (16). The next transformation

$$\eta = 2^{1/2}\sin(\phi/2),$$
$$\zeta = t\cdot\eta(\phi)/t_0(\phi) \qquad (26)$$

leads to formula (9) with the weighting function

$$w(\eta,\zeta) = 2/[2-(1-\eta^2)^2]^{1/2}. \qquad (27)$$

Transformation reciprocal to (26) and (17)

$$\cos\phi = 1-\eta^2,$$
$$\cos\theta = \zeta\cdot\{[2-\eta^2]/[2-(1-\eta^2)^2]\}^{1/2} \qquad (28)$$

allows one to express $\hat{\vec{r}}$ (24) as a function of (η,ζ). We note, that the transformation (19) used instead of (26) for tetragonal crystals would lead to the weighting function singular at the boundary of integration region.

2.2.3. Hexagonal Crystals

The symmetry-irreducible angle equals

$$\Omega_{ir} = 4\pi/24. \qquad (29)$$

and is characterized by vectors:

$$\vec{Q}_1 = (1,0,0),\ \vec{Q}_2 = (3^{1/2}/2, 1/2, 0),\ \vec{Q}_3 = (0,0,1), \qquad (30-$$

where the z direction is along the 6-fold axis and the x direction perpendicular to the mirror plane. In order to derive the formula (9) by means of the spherical transformation, we again use (24) and (17) and obtain (25), where $t_0(\phi)$ is defined now by the condition $\hat{y} = \hat{x}/3^{1/2}$, which gives

$$t_0(\phi) = \sin\phi/(3 + \sin^2\phi)^{1/2}. \tag{31}$$

Next, the transformation (19) leads to the final formula (9) with the weighting function

$$w(\eta, \zeta) = 2/[4 - (1 - \eta^2)^2]^{1/2}, \tag{32}$$

while the reciprocal transformation

$$\cos\phi = 1 - \eta^2,$$
$$\cos\theta = \zeta \cdot \{[2 - \eta^2]/[4 - (1 - \eta^2)^2]\}^{1/2} \tag{33}$$

allows one to express $\hat{r}$ (24) as a function of (η, ζ).

2.2.4. Trigonal Crystals

We choose the symmetry-irreducible angle

$$\Omega_{ir} = 4\pi/12 \tag{34}$$

defined by the vectors

$$\vec{Q}_1 = (1,0,0), \quad \vec{Q}_2 = (1/2, 3^{1/2}/2, 0), \quad \vec{Q}_3 = (0,0,1). \tag{35}$$

The derivation of (9) by means of the spherical transformation goes as in the previous case, but $t_0(\phi)$ is defined now by the condition $\hat{y} = \hat{x} \cdot 3^{1/2}$ which gives:

$$t_0(\phi) = \sin\phi/(1/3 + \sin^2\phi)^{1/2}. \tag{36}$$

The weighting function w for the formula (9) is

$$\dot{w}(\eta, \zeta) = 2/[4/3 - (1 - \eta^2)^2]^{1/2} \tag{37}$$

and the reciprocal transformation

$$\cos\phi = 1 - \eta^2,$$
$$\cos\theta = \zeta \cdot \{[2 - \eta^2]/[4/3 - (1 - \eta^2)^2]\}^{1/2}. \tag{38}$$

2.3. Numerical Tests

In order to check the accuracy of our method and to compare the efficiency of different our approaches as well as to compare our results with recently published methods /1/, we have performed a series of calculations.

The direction average (3) was calculated in the case of four symmetry-irreducible regions considered above. For cubic and tetragonal crystals, as the averaged functions there were taken some cubic invariant polynomials:

$$f_1 = 1,$$
$$f_2 = \hat{x}^2\hat{y}^2 + \hat{y}^2\hat{z}^2 + \hat{z}^2\hat{x}^2,$$
$$f_3 = \hat{x}^4 + \hat{y}^4 + \hat{z}^4, \tag{39}$$
$$f_4 = \hat{x}^2\hat{y}^2\hat{z}^2,$$
$$f_5 = \hat{x}^4\hat{y}^2 + \hat{x}^2\hat{y}^4 + \hat{y}^4\hat{z}^2 + \hat{y}^2\hat{z}^4 + \hat{z}^4\hat{x}^2 + \hat{z}^2\hat{x}^4.$$

Four of them (besides the first one) are identical with the functions $O_{2,2}$, O_4, $O_{2,2,2}$, $O_{4,2}$ used for the test in /1/ (where the discussion of their anisotropy may be found).

For tests in hexagonal and triagonal crystals, some cylindrical invariant polynomials were taken:

Table I

№	Sym-metry	Method of integration				Relative errors of				
		transf.	N_{div}	N_{deg}	N_{tot}	$\langle f_1 \rangle$	$\langle f_2 \rangle$	$\langle f_3 \rangle$	$\langle f_4 \rangle$	$\langle f_5 \rangle$
1	cub.	spher.	1	5	7	-9.3E-5	2.0E-4	-2.9E-4	-1.8E-3	5.4E-4
2	cub.	linear	1	5	7	2.4E-4	1.2E-3	-3.8E-4	-9.7E-3	3.0E-3
3	cub.	spher.	2	5	28	-4.9E-6	5.7E-7	-8.5E-6	-1.3E-5	2.8E-6
4	cub.	linear	2	5	28	1.2E-6	1.6E-5	8.6E-6	2.0E-5	1.5E-5
5	tetr.	spher.	2	5	28	-1.9E-6	1.2E-4	-8.2E-5	-1.9E-4	1.7E-4
6	hex.	spher.	2	5	28	-3.8E-7	-1.0E-5	4.6E-6	9.8E-5	-3.6E-5
7	trig.	spher.	2	5	28	-1.7E-5	-1.7E-4	6.2E-5	3.2E-4	1.4E-4
8	cub.	spher.	4	5	112	-1.4E-7	-1.5E-8	-2.3E-7	-1.4E-7	5.4E-9
9	cub.	linear	4	5	112	1.9E-8	1.1E-7	-4.3E-8	-9.6E-9	1.3E-7
10	cub.	linear	22	1	484	1.5E-4	2.2E-4	1.0E-4	1.0E-4	2.4E-4
11	cub.	spher.	22	1	484	-6.7E-5	-4.4E-5	-8.3E-5	-2.8E-4	-4.5E-6
12	cub.	spher.	12	2	432	-3.5E-7	-6.1E-9	-5.8E-7	1.4E-6	-2.4E-7
13	cub.	spher.	8	5	448	-2.9E-9	-4.9E-10	-4.6E-9	-1.6E-9	-2.9E-10
14	cub.	linear	8	5	448	2.9E-10	1.7E-9	-6.2E-10	-3.5E-10	2.0E-9
15	tetr.	linear	8	5	448	-1.5E-9	-2.6E-9	-7.6E-10	-7.5E-10	-2.9E-9
16	hex.	linear	8	5	448	-2.1E-9	6.9E-9	-6.6E-9	5.4E-9	-4.8E-9
17	trig.	linear	8	5	448	-3.4E-10	1.1E-8	-6.1E-9	-9.9E-9	3.2E-9
18	cub.	UVD [1]	-	-	489	0	3.7E-5	-2.4E-5	-1.4E-4	6.6E-5

$$
\begin{aligned}
f_1 &= 1, \\
f_2 &= \hat{z}^2, \\
f_3 &= \hat{x}^2 + \hat{y}^2, \\
f_4 &= \hat{z}^2 (\hat{x}^2 + \hat{y}^2), \\
f_5 &= \hat{z}^2 + (\hat{x}^2 + \hat{y}^2)^2 ;
\end{aligned}
\tag{40}
$$

The obtained results are presented in *Table 1* in the form of relative errors of the averages $\langle f_i \rangle$ (with respect to the exact values, obtained analytically). The three methods are compared: two our methods, the first based on linear transformation (7) and the second - on spherical transformation (14) or (24), and the uniform vector distribution (UVD) method of Overton and Schuch /1/. The total number of points at which integrand was calculated is designated as N_{tot}. The parameters N_{div} and N_{deg} were described at the end of chapter 2.1.

High efficiency of our method is demonstrated in the best way by example No. 14, in comparison with No.18: at comparable (though less) number of sampling points our results are more accurate by 4-5 orders of magnitude. This is achieved owing to Hammer's integration formula of the 5th degree polynomial accuracy. Really, if we apply our method together with $N_{deg} = 1$ (see, No. 10, 11), then at comparable number of points, the accuracy is roughly the same as Overton's one (No. 18). It is easy to explain, because Overton's uniform distribution of points assures the 1st degree polynomial accuracy.

By comparison of No. 3 and 4 with 18 we demonstrate the efficiency of our methods in another way. Our results, slightly better than Overton's one, are obtained using the 28-point formula, while his - by the 489-point formula.

What concerns the comparison between our methods based on spherical and linear transformation, we demonstrate it for the cubic symmetry, see examples 1 and 2,

3 and 4, 8 and 9, 13 and 14, 11 and 10. Spherical transformation method gives slightly better results in the case of small number of sampling points (No. 1 and 2) or low N_{deg} (No. 11 and 10), what is connected with smoother weighting function. In the remaining cases both methods give a comparable accuracy. The same rule was observed by us for other symmetries. Taking also into account the fact that in the spherical transformation method more computer time is necessary to calculate the coordinates and weights, and that it must be programmed separately for each symmetry, we choose the method based on linear transformation as worthly of practical applications.

Comparing examples 11, 12 and 13 we can see how the accuracy increases with increasing N_{deg} at almost constant level of N_{tot}. On the other hand, keeping integration formula fixed, the accuracy practically does not depend on magnitude of irreducible angle (or symmetry), what is demonstrated by a series of examples No. 14, 15, 16, 17 and No. 3,5,6,7.

3. *INTEGRATION OVER THE VOLUME*

3.1. *General Formula*

Let us consider the average

$$\langle\langle F \rangle\rangle = \frac{1}{V_{BZ}} \int_{BZ} d^3k\, F(\vec{k}) \tag{41}$$

of the function F over the volume of the Brillouin Zone. We assume the function F to possess the crystal symmetry, and therefore, it would be enough to integrate over the smaller region, the symmetry-irreducible volume V_{ir}, a rather complicated polyhedron, depending on the symmetry considered. Nevertheless, it is easy to develop the general method of integration if we decompose the region V_{ir} into the simplest subregions, tetrahedrons. First, we observe, that V_{ir} can be represented as a sum of pyramids, which bases are parts of the BZ boundary faces and which common vertex is the center of coordinate system. If bases are triangles, we have already tetrahedrons; other bases always can be decomposed into triangles. (Below we shall give the examples of such decompositions for a few common symmetries).

So the average (41) can be rewritten as

$$\langle\langle F \rangle\rangle = \sum_{j=1}^{n_s} \frac{V^{(j)}}{V_{ir}} \langle\langle F \rangle\rangle_j , \tag{42}$$

where n_s is the number of tetrahedrons into which V_{ir} is decomposed, and where

$$\langle\langle F \rangle\rangle_j = \frac{1}{V^{(j)}} \int_{V^{(j)}} d^3k\, F(\vec{k}) \tag{43}$$

is the average over the j-th tetrahedron $V^{(j)}$.

Figure 1 will serve again as the illustration of a typical tetrahedron OABC. We can take advantage of our experience with solid angle integration if we represent the volume element as

$$d^3k = d^2\Omega \cdot k^2 \cdot dk . \tag{44}$$

Then

$$\langle\langle F \rangle\rangle_j = \frac{1}{V^{(j)}} \int_{\Omega^{(j)}} d^2\Omega \int_0^{|\vec{r}|} k^2 dk\, F(k\hat{\vec{r}}), \tag{45}$$

where $\vec{r}$ is the point laying on the base ABC, and therefore given by form. (7). After introducing the dimensionless radius

$$\xi = k/|\vec{r}| \tag{46}$$

and using (5), (8), (9) we rewrite (45) in the form

$$\langle\langle F \rangle\rangle_j = W_j \int_0^1 d\eta \int_0^{\eta} d\zeta \int_0^1 d\xi \cdot \xi^2 \cdot F(\vec{k}^{(j)}(\xi, \eta, \zeta)) , \tag{47}$$

where

$$\vec{k}^{(j)} = \xi \cdot (\vec{K}_1^{(j)} + \eta \vec{K}_2^{(j)} + \zeta \vec{K}_3^{(j)}) , \tag{48}$$

$$W_j = [\vec{K}_1^{(j)} \cdot (\vec{K}_2^{(j)} \times \vec{K}_3^{(j)})]/V^{(j)}. \quad (49)$$

The last quantity may be calculated immediately

$$W_j = 6. \quad (50)$$

So the average over tetrahedron (47) was reduced to the one-dimensional integral over ξ on the interval $[0,1]$ and the two-dimensional integral over (η, ζ) on the triangle $\{(0,0), (1,0), (1,1)\}$.

As in the case of solid angle integration, a high accuracy of numerical procedure will be achieved when the methods of high polynomial accuracy will be involved. So, the integral over triangle will be taken as previously, while the integral over the interval will be taken by means of Gauss' method, in which the N_p-point formula assures polynomials of at most $N_{deg} = (2N_p - 1)$ degree to be integrated exactly. As previously the unit interval may be preliminary decomposed into N_{div} equal subintervals, if necessary.

In the Hammer's and Stroud's paper (ref. /6/ tab. I) one can find the integration formulae for squares, similar to those for triangles, like eq. (11), quoted earlier (now $N_{deg} = 1, 3, 5, 7$ with corresponding $N_p = 1, 4, 9, 12$). This allows us to treat in representation (42) as elementary subregious not only tetrahedrons, but also the pyramids with parallelogram base (which is equivalent to square through affine transformation). Examples of such subregions will be given below. In the case of using them, the form. (47) is to be slightly changed in that sense, that in the integral over ζ the upper limit must be 1, instead of η, i.e., the integration over (η, ζ) is to be performed on the unit square now. This leads to a new value of the coefficient W_i in (47), namely

$$W_j = 3. \quad (51)$$

The paper of Hammer et al. (ref. /5/ page 136), quoted earlier, gives also integration formulae directly

for tetrahedron, exact for quadratic and cubic polynomials, involving 4 and 5 points of evaluation, affine-symmetrically distributed over the tetrahedron. These formulae may be applied to (43) immediately, giving the integration formula with very low number of sampling points. It may be very useful in those cases, when crude results are sufficient.

We shall not exploit this possibility in our further application for the two reasons. First, it should be necessary to decompose the tetrahedron into smaller and equal tetrahedrons, in order to increase accuracy. But this can not be done in the unique way (as was possible in the case of interval and triangle) and therefore it would introduce arbitrariness into the algorithm. Second, when the function of the phonon spectrum $\omega_i(\vec{k})$ is to be averaged, polynomials do not approximate it well, because it is not the analytical function of $\vec{k}$ at $\vec{k} = 0$ (but it is the analytical function of $|\vec{k}|$, which favours the formulae (45) and (47)).

3.2. Application to Crystals of Different Symmetries

3.2.1. The Simple Cubic Lattice (SC)

The BZ for this lattice is a cube, which symmetry-irreducible region is a tetrahedron. The triangular base of it is 1/8 of the square face of BZ. *Table II* contains all the data necessary to perform calculations according to (42), (47).

3.2.2. The Body Centered Cubic Lattice (BCC)

The BZ is a regular dodecahedron, which rhombic faces are perpendicular to (110) (and equivalent) directions. The symmetry-irreducible region is a tetrahedron, which base is 1/4 of one of the BZ faces. See *table II* for details.

Table II

Vectors and coefficients describing the subregions of integration for some crystal lattices

Latt.	n_s	j	$K_1^{(j)}$	$K_2^{(j)}$	$K_3^{(j)}$	W_j	$V^{(j)}/V_{tr}$
SC	1	1	(1/2, 0, 0)	(0, 1/2, 0)	(0, 0, 1/2)	6	1
BCC	1	1	(1, 0, 0)	(-1/2, 1/2, 0)	(0, 0, 1/2)	6	1
FCC	3	1	(1, 1/2, 0)	(0, -1/4, 1/4)	(0, -1/4, -1/4)	6	2/8
		2	(1, 1/2, 0)	(-1/4, 1/4, 0)	(-1/4,-1/4, 1/2)	6	3/8
		3	(1, 1/2, 0)	(-1/2, 0 , 1/2)	(1/2,-1/4 , -1/4)	6	3/8
HCP	2	1	(0, 0, a/(2c))	(0, $-1/\sqrt{3}$, 0)	(1/3, 0, 0)	6	1/3
		2	(0, $-1/\sqrt{3}$, 0)	(1/3, 0, 0)	(0, 0, a/(2c))	3	2/3
Tric	3	1	[1/2, -1/2, -1/2]	[0, 1, 0]	[0, 0, 1]	3	1/3
		2	[-1/2, 1/2, -1/2]	[0, 0, 1]	[1, 0, 0]	3	1/3
		3	[-1/2, -1/2, 1/2]	[1, 0, 0]	[0, 1, 0]	3	1/3
Rhh	1	1	[-1/2, -1/2, 1/2]	[1, 0, 0]	[0, 1, 0]	6	1

Note: In the case of $W_j = 3$ the integration over (ξ, ζ) in (47) must be extended to the unit square. Vector coordinates in the round brackets are given in the Cartesian system, in units of $(2\pi/a)$; coordinates in the square brackets - in the reciprocal lattice vector system.

3.2.3. The Face Centered Cubic Lattice (FCC)

Its BZ boundary consists of 6 quadratic faces (perpendicular to the 4-fold axes) and of 8 hexagonal ones (perpendicular to the 3-fold axes). Therefore the symmetry-irreducible region may be represented as the sum of one tetrahedron (which triangular base is 1/8 of the square face; denoted by $j = 1$ in *Table II*) and of one pyramid (which tetragonal base is 1/6 of the hexagonal face). The latter is decomposed into two tetrahedrons ($j = 2,3$).

3.2.4. The Hexagonal Close Packed Lattice (HCP)

The BZ is a hexagonal prism, which two bases are perpendicular to the 3-fold axis, while six sides are perpendicular to the bases. The symmetry-irreducible region consists of one tetrahedron (which triangular base is 1/12 of the hexagonal face; $j = 1$ in *Table II*) and of one rectangular pyramid (which base is 1/4 of the BZ side; $j = 2$).

3.2.5. The Triclinic Lattice

The BZ considered in the previous, high-symmetrical lattice cases, was constructed according to the usual rule, requiring each BZ face to be perpendicular to some reciprocal lattice vector. This rule when applied to low-symmetrical lattices would lead to the BZ surface consisitng of a great number of pieces, exhibiting no symmetry. Therefore we prefer to average over the following region having, as the BZ, the property of contributing all inequivalent points of $\vec{k}$-space, namely the parallelepiped built up on the three elementary reciprocal lattice vectors, and then shifted in order to situate in its center the center of coordinate system. Supposing the integrand to possess the inversion symmetry

(as it usually occurs in the solid state applications) the symmetry-irreducible region consists of three pyramids with parallelogram bases (see *Table II*).

3.2.6. The Rhombohedral Lattice (Rhh)

We choose the same averaging region as in the previous case, but the symmetry-irreducible part of it consists now of one tetrahedron, which base is 1/2 of the parallelogram face (see *Table II*).

3.3. The Numerical Test. The Calculation of the Phonon Spectrum Moments

In order to demonstrate efficiency of our method, we performed the calculations of some moments of the typical phonon spectrum of the crystal having HCP lattice. We choose phonon dispersion relations $\omega_i(\vec{k})$ of molecular hydrogen at zero pressure, measured by Nielsen /7/ and parametrized by him within the Born-Karman third-nearest-neighbour force model. We have calculated the average over the branches and over BZ:

$$\langle\langle\omega^{\ell}\rangle\rangle = \langle\langle \frac{1}{6}\sum_{i=1}^{6}(\omega_i)^{\ell}\rangle\rangle . \qquad (52)$$

The results are demonstrated in *Table III* in the form of relative errors of the mentioned quantities for $\ell = -1,1,2,3$. The exact value of $\langle\langle\omega^2\rangle\rangle$ has been found analytically, which is possible in the case of the Born-Karman model. For other momenta the values obtained in calculation No. 1 (using more than 30 thousands of points) served us as "almost exact" for the calculation of the relative errors. The error of $\langle\langle\omega^2\rangle\rangle$ assures us that it is a reasonable assumption. The values of calculated momenta (rounded to four digits) are the following: $\langle\langle\omega^{-1}\rangle\rangle = 0.1659$, $\langle\langle\omega\rangle\rangle = 6.727$, $\langle\langle\omega^2\rangle\rangle = 48.69$, $\langle\langle\omega^3\rangle\rangle = 372.0$, ω in units of *meV*.

Table III

No	Integr. param.			Relative errors of			
	N_{div}	N_{deg}	N_{tot}	$\langle\langle\omega^{-1}\rangle\rangle$	$\langle\langle\omega\rangle\rangle$	$\langle\langle\omega^2\rangle\rangle$	$\langle\langle\omega^3\rangle\rangle$
I	8	5[a]	32768	—	—	I.9E-II	—
2	4	5	3072	-I.0E-7	-2.8E-8	-9.0E-8	-I.3E-7
3	3	5	I296	-2.7E-7	-2.3E-7	-5.3E-7	-7.2E-7
4	2	5	384	6.9E-6	-4.4E-6	-6.7E-6	-7.7E-6
5	I	5	48	3.IE-4	-3.5E-4	-9.2E-4	-8.2E-4
6	4	3	I024	4.IE-7	2.4E-5	2.9E-5	4.9E-5
7	2	3	I28	-I.5E-5	4.3E-4	5.5E-4	8.6E-4
8	I	3	I6	-3.8E-3	I.IE-2	I.9E-2	2.3E-2
9	8	I	I024	I.3E-3	-5.0E-4	-9.0E-4	-I.2E-3
I0	4	I	I28	5.2E-3	-2.IE-3	-3.8E-3	-5.3E-3

a) In this case the integral along the radius ξ has been calculated with $N_{deg} = 7$.

Table III demonstrates that even at small number of sampling points the results are of interest, e.g., the 16-point integration gives a few percent accuracy (No. 8), the 48-point integration - accuracy better than one part in 10^3 (No. 5), and so on, up to the accuracy of one part in 10^7 at 3 thousands of points (No. 2).

At fixed total number of sampling points N_{tot}, the calculation with higher degree of polynomial accuracy N_{deg} gives noticeably better results (compare No. 10 with 7, also 9 with 6 and 3). It is well demonstrated in *Fig. 2*, where relative errors ϵ of $\langle\langle\omega^2\rangle\rangle$ versus N_{tot} are plotted for the three different N_{deg}. We see that the calculated points lay fairly well on lines

$$\epsilon = C \cdot N_{tot}^{-(N_{deg}+1)/3} \qquad (53)$$

with coefficient C of the order of one.

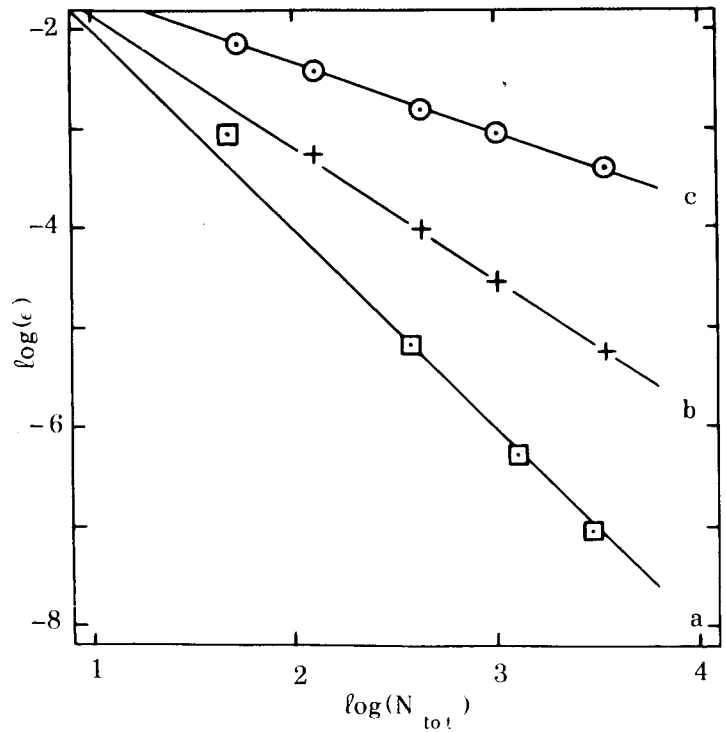

Fig. 2. The relative error ϵ *of* $\langle\langle\omega^2\rangle\rangle$ *vs the total number of sampling points* N_{tot}. *Points calculated according to the integration formula with* N_{deg} *= 5,3 and 1 are denoted by* □ , + *and* ○ , *respectively. Line* a *represents* $\epsilon \sim N_{tot}^{-6/3}$, , b – $\epsilon \sim N_{tot}^{-4/3}$ *and* c – $\epsilon \sim N_{tot}^{-2/3}$.

The dependence (53) is a three-dimensional analog of the error formula in Gauss' method. It is interesting, that the calculated errors are well described by (53) even for small values of N_{tot} , as it can be seen from *Fig. 2.*

3.4. Integration with the Density of Points Increasing towards the Center of BZ

In the examples of integration over BZ considered above the integrands at different points of BZ were of the same order of magnitude. But calculating some thermodynamic properties (e.g., specific heat $C_V(T)$) one can find quite a different situation. The integrand is practically zero beyond some region around the center. The dimensions of this region diminish with decreasing temperature, and become small compared to the dimensions of the BZ for temperatures much smaller than the Debye temperature. In order to integrate efficiently such functions, using the same formula both for high and low temperatures, the employed density of sampling points must strongly increase towards the center of BZ.

In paper /2/ this problem was considered in detail and two methods, obeying the stated requirement, were developed: the concentric region method (CRM) and the Gauss method (GM).

Our formula (47) for the integration over BZ may be easily generalized to the form equivalent to CRM. Namely, performing the integration over ξ along the radius, we decompose now the interval $[0, 1]$ into N subintervals, which lengths decrease towards the beginning (instead of the equal subintervals as used previously):

$$[0,1] = [0, p^{N-1}] + [p^{N-1}, p^{N-2}] + [p^{N-2}, p^{N-3}] + \ldots + [p^1, p^0], \quad (54)$$

where the parameter p describes the ratio of the scalling down, $p < 1$. All other prescriptions remain the same, i.e., to each subinterval Gauss' formula is applied, and to the integrals over (η,ζ), Hammer's formula.

Notice, that our approach is applicable immediately to any symmetry (while methods of ref. /2/ suited FCC and SC lattices only) and there are no any troubles with consideration of many kinds of subzones, description of which filled up a few pages of paper /2/.

In order to compare the efficiency of our method with methods of ref. /2/, we have performed a numerical test, evaluating the function

$$C(\theta) = \langle\langle \left(\frac{x}{\sinh x}\right)^2 \rangle\rangle , \quad (55)$$

where

$$x = (a/2\pi)|\vec{k}|/\theta$$

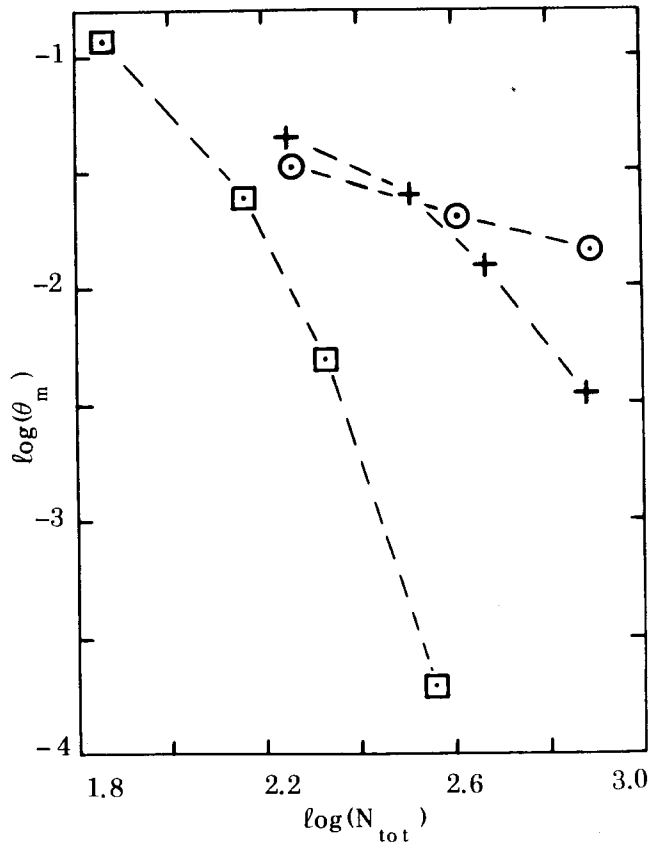

Fig. 3. The limiting temperature θ_m vs the total number of sampling points N_{tot}. Points from our calculations are denoted by □; from ref. /2/ according to CRM - by +, to GM - by ○.

the same as in ref. /2/ form. (47). Calculation of $C(\theta)$ simulates the evaluation of specific heat, the parameter θ means temperature in units of the Debye temperature.

Calculations were performed for the FCC lattice; the integral over (η, ζ) was taken according to 3-point Hammer's formula (applied to each of the three triangles -

see Chapter 3.2.4 and *Table II*); the scalling factor was chosen $p = 0.2$, the number of subintervals $N = 1,2,3,5$, the integration over each subinterval according to 4-point Gauss' formula, applied twice (to each half of a subinterval). So the total number of the sampling points was $N_{tot} = 72, 144, 216, 360$, respectively.

At each case of N we were looking for the minimal temperature θ_m, satisfying the condition, that for temperatures $\theta > \theta_m$, the function $C(\theta)$ is calculated with sufficient accuracy, i.e., with a relative error less than 0.2%.

Our results are demonstrated on *Fig. 3*, together with the results of ref. /2/, taken from their *Fig. 2*. One immediately sees that our method allows one to calculate a specific heat at lower temperatures and at a smaller number of sampling points. Though geometrically it is completely equivalent to CRM of /2/, it owes its higher efficiency to Gauss' and Hammer's formula of integration, as it was observed already in the previous examples of our work.

4. SUMMARY

The evaluation of solid angle integral over the symmetry-irreducible part of BZ is reduced to the evaluation of the integral over a triangle. The variable transformation and weighting function involved are easy to be programmed. There are given examples of the geometrical information allowing one to apply this transformation to crystals of cubic, tetragonal, hexagonal and triagonal symmetry. The numerical tests convincingly demonstrate high efficiency of the method, if Hammer's formula /5/ of high degree polynomial accuracy is used for the evaluation of the integral over a triangle.

For the volume integration the BZ should be decomposed preliminary into elementary subregions, tetrahedrons. This procedure, together with all necessary geometrical information is demonstrated by examples given for ST, BCC, FCC, HCP, rhombohedral and triclinic structures. The integral over any tetrahedron is repre-

sented as the integral over a standard triangle and the integral over the unit interval. If the first one is evaluated according to Hammer's formula[5], and the second - to Gauss' formula, then, as it is shown by numerical tests, a rapid convergence is obtained.

Within our method it is easy to construct the formula with increasing density of sampling points towards the center of BZ, necessary for same thermodynamic calculations.

REFERENCES

1. *W.C.Overton, Jr., and A.F.Schuch. J.Computational Phys., 14, 59 /1974/.*
2. *R.J.Hardy, J.W.Morrison and S.Bijanki. J.Computational Phys., 13, 591 /1973/.*
3. *F.M.Mueller, J.W.Garland, M.H.Cohen. and K.H.Benneman. Ann.Phys., 67, 19 /1971/.*
4. *D.Brust. Phys.Rev., 134, A1337 /1964/.*
5. *P.C.Hammer, O.J.Marlowe and A.H.Stroud. M.T.A.C., 10, 130 /1956/.*
6. *P.C.Hammer and A.H.Stroud. M.T.A.C., 12, 272 /1958/.*
7. *M.Nielsen. Phys.Rev., B7, 1626, 1/1973/.*

Received by Publishing Department on February 2, 1976.